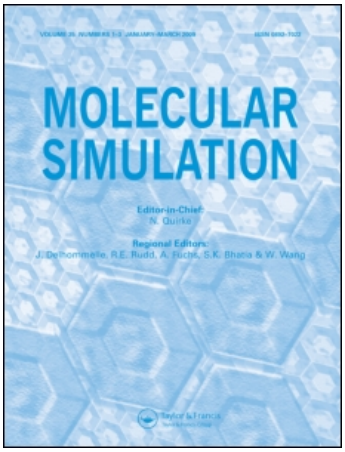

Molecular Simulation
Publication details, including instructions for authors and subscription information:
http://www.informaworld.com/smpp/title~content=t713644482

Effect of Cation Concentration on Molecular Dynamics Simulations of UDP-Glucose

Pavla Petrová[a]; Jaroslav Koča[a]; Anne Imberty
[a] Laboratory of Biomolecular Structure and Dynamics, Masaryk University, Brno, Czech Republic

To cite this Article Petrová, Pavla , Koča, Jaroslav and Imberty, Anne(2000) 'Effect of Cation Concentration on Molecular Dynamics Simulations of UDP-Glucose', Molecular Simulation, 24: 4, 325 — 340
To link to this Article: DOI: 10.1080/08927020008022379
URL: http://dx.doi.org/10.1080/08927020008022379

Molecular Simulation, 2000, Vol. 24, pp. 325–340
Reprints available directly from the publisher
Photocopying permitted by license only

EFFECT OF CATION CONCENTRATION ON MOLECULAR DYNAMICS SIMULATIONS OF UDP-GLUCOSE

PAVLA PETROVÁ[a,b], JAROSLAV KOČA[a] and ANNE IMBERTY[b,*]

[a] *Laboratory of Biomolecular Structure and Dynamics, Masaryk University, Kotlárská 2, 611 37 Brno, Czech Republic;* [b] *CERMAV-CNRS, BP 53, F-38041 Grenoble cedex 9, France, Associated with University Joseph Fourier*

(Received April 1999; accepted May 1999)

Glycosyl esters of nucleoside di or mono-phosphates, generally referred to as "sugar nucleotides", serve as a sugar donors during the biosynthesis of oligo- and polysaccharides; they are therefore of a primary importance in carbohydrate metabolism in the living world. Molecular dynamics simulations were used to explore the conformational flexibility of one nucleotide sugar, UDP-glucose (UDP-Glc). The AMBER program package was used with some new parameters especially developed for nucleotide sugars. Several simulations on this molecule in aqueous solution, each of 2 ns duration, were carried out for increasing concentrations of monovalent K^+ and divalent Mg^{2+} ions. For the monovalent ion, it is revealed that its presence and concentration is crucial for the conformational behavior, resulting in the stabilization of the extended conformation. The preferred location of K^+ is in close proximity to the negatively charged phosphate oxygens, but the ion moves freely and can occupy other sites. Since the size of this cation is close that of the water molecules, the hydration scheme is not perturbed. Completely different results are obtained when the divalent Mg^{2+} cation is introduced in the simulation. A very strong interaction is established between the phosphate group and the cation; as a result the UDP-Glc molecule is locked in a rigid extended geometry. The analyses of the trajectories provide new insight on the role of the metal ion in the catalytic mechanism of glycosyltransferases.

Keywords: Molecular dynamics; UDP-glucose; nucleotide-sugar

*Corresponding author.

INTRODUCTION

Glycosyl esters of nucleoside di- or mono-phosphates, generally referred to as "sugar nucleotides", are of a primary importance in carbohydrate metabolism [1]. These activated sugars act as donors during the biosynthesis of oligosaccharides, polysaccharides and glycoconjugates in the living world [2]. The most important nucleotide-sugars involved in the biosynthetic pathway of mammalian N-glycans are UDP-glucose (UDP-Glc), UDP-N-acetyl-glucosamine (UDP-GlcNAc), GDP-mannose (GDP-Man), GDP-fucose (GDP-Fuc) and CPM-sialic acid (CMP-NeuAc). As a result of the development of chemo-enzymatic methods in the field of carbohydrate synthesis, nucleotide-sugars have become substrates of great interest in the synthesis of pharmaceutical oligosaccharides.

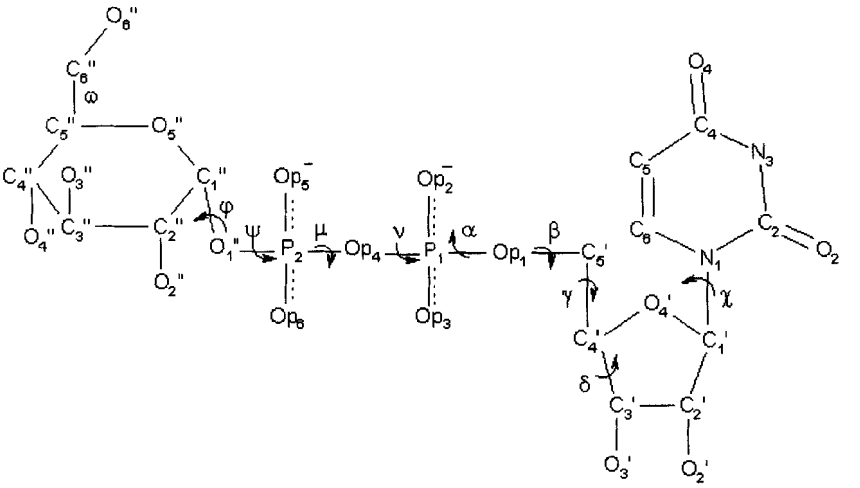

Schematic representation of UDP-glucose with labeling of the atoms and torsion angles of interest.

Our present knowledge about the structure of nucleotide-sugars is very limited. Only one crystal structure of the sodium salt of UDP-Glc [3] has been solved. Two recent theoretical studies investigated the conformational behavior of the sugar-phosphate linkage at the *ab-initio* level [4, 5]. From these calculations, our group proposed energy parameters to be used in AMBER [6, 7] for the conformational study of nucleotide-sugars. Using the CICADA program [8] together with this new parameterization for the AMBER force-field, exploration of the conformational space of two nucleotide-sugars, *i.e.*, UDP-Glc and GDP-Fuc, demonstrated the high

flexibility of these molecules [4]. The multitude of possible conformations can be clustered in a limited number of overall shapes for theses molecules. These shapes were given names according to their similarities with alphabetic letter: *i.e.*, U or V for folded shapes, S or L for more extended ones. Because this preliminary conformational study was conducted with no explicit water molecules, the folded shapes were favored in energy.

In order to better understand the conformational behavior of nucleotide-sugars, it is necessary to include explicit water molecules, together with appropriate counter-ions. Both the concentration and the nature of the counter-ion can influence the conformation of the nucleotide-sugar. The interactions between the nucleotide-sugar and the cation could have some important biological effect. It is known that many glycosyltransferases absolutely require the presence of a metal cofactor. For example, the fucosyltransferase FucT V has a preference for metal ions that can adopt an octahedral geometry and operates optimally with Mn^{2+} [9]. In fact, the effect of divalent cation is very general since Mn^{2+} alone is responsible for the nonenzymatic hydrolysis of GDP-Fuc. As for glucosyltransferases and galactosyltransferases, biochemical studies [10], together with sequence analysis [11] and molecular modeling [12], suggest that the divalent cation is necessary in the protein/nucleotide sugar interaction, as a bridge between acidic amino acids (usually in a DXD motif) and the phosphate group of the nucleotide-sugar.

We report here the first simulations of nucleotide-sugars in water environment and in the presence of several concentrations of mono- and divalent cations. The analyses of the trajectories provide new insight on the role of the metal ions in the catalytic mechanism of glycosyltransferases.

COMPUTATIONAL METHODS

Simulations were performed using the AMBER-5.0 program package with several new parameters especially developed for nucleotide sugars [4]. K^+ and Cl^- van der Waals parameters have recently been introduced into the parm94 file of standard parameters; for Mg^{2+} the Aquist parameters [13] were used. The X-ray derived structure [3] was used as a starting geometry and the topology file was constructed as described before [4]. Explicit potassium and magnesium counterions were placed nearby the phosphate groups by the Xleap module of AMBER. This program iteratively positions each of the ions about a solute at the point of next lowest electrostatic potential. We considered four concentrations of ions: without ions, low,

medium and high salt concentration (see Tab. I). The number of Cl^- ions was adjusted to maintain the neutrality of the system. The solute together with counterions were hydrated by a periodic box of TIP3P waters which extended approximately 10 Å in each direction from the nucleotide sugar atoms.

All simulations were run with the SANDER module of AMBER-5.0 with SHAKE algorithm [14] (tolerance = 0.0005 Å) to constrain covalent bonds involving hydrogens, using periodic boundary conditions, a 2 fs time step, a temperature of 300 K with Berendsen temperature coupling [15], a 9 Å cutoff applied to the Lennard-Jones interaction, and constant pressure $P = 1$ atm. The nonbonded list was updated every 10 steps.

Equilibration was performed by first restraining the atoms of the UDP-Glc (water molecules were allowed to move) and running 1000 steps of minimization. After this initial minimization, all subsequent simulations were run by using the particle mesh Ewald method (PME) [16] within AMBER-5.0 with a cubic B-spline interpolation order and a 10^{-6} tolerance for the direct space sum cutoff. To speed up the fast Fourier transform in the calculation of the reciprocal sum, the size of the PME charge grid was chosen to be a product of powers of 2, 3 and 5 and to be slightly larger then the size of the periodic box. This leads to a grid spacing of ~1 Å or less. The first step was followed by dynamics for 25 ps with the position of the UDP-Glc fixed. Equilibration was continued with 25 kcal/(mol·Å^2) restraints placed on all solute atoms, minimization for 1000 steps, followed by 3 ps of MD, which allowed the water to relax around the solute. This equilibration was followed by 5 rounds of 600-steps minimization where the solute restraints were reduced by 5 kcal/(mol·Å^2) during each round. Finally, the system was heated from 100 to 300 K over 2 ps and the production runs were initiated.

The MD trajectories were analyzed with the CARNAL module of AMBER (torsions, distances) and the adapted trajectory analysis software RDPARM (radial distribution functions).

TABLE I Number of cations and water molecules in each MD simulation

Name of the simulation	K^+	Mg^{2+}	Cl^-	*Water molecules*
NO	–	–	–	890
LOW_K	2	–	–	1168
MEDIUM_K	6	–	4	1719
HIGH_K	12	–	10	1978
LOW_Mg	–	1	–	955
MEDIUM_Mg	–	3	4	1415

RESULTS

Six MD simulations were run using the X-ray derived geometry as the starting point. The ion concentrations and the number of water molecules in the system are shown in Table I.

Simulation in the Presence of Increasing Concentration of Monovalent Cations

Analysis of the Conformation

Fluctuations of the root mean square from the starting X-ray structures have been monitored during each of the 2 ns trajectories (Fig. 1) and the averaged values were calculated over last 1.5 ns of each trajectory (Tab. II). In all cases, averaged RMS values lie between 0.08 and 0.8 Å, indicating that the molecule does not stay in its starting semi folded conformation. Diphosphate fluctuations are the largest, which is in agreement with the high flexibility of these linkages, followed by the ribose and glucose moieties. The mobility of the base seems to be independent of the concentration and the valence of the cation. Comparison of the simulations with and without ions indicates that the mobility of the diphosphate backbone decreases in the presence of the salt.

The mobility of individual torsions was also analyzed (Fig. 1). More frequent fluctuations occur for the μ and ν torsional angles that adopt the three staggered orientations, for all concentrations in monovalent counterion (not displayed). The ribose ring starting structure is C2-endo but both puckering modes, *i.e.*, C2-endo and C3-endo, are visited during all MD simulations in the presence of monovalent cations. As for the other torsion angles, fluctuations among the possible orientations previously predicted by the exploration of the conformational space [4] are observed, usually on time scale of a few hundredths of ps. For the highest concentration in salt, some of the torsion angles have a less flexible behavior. For example, it can be observed that the α torsion angle remains trapped in the gauche+ orientation throughout the HIGH_K simulation. Nevertheless, for most of the torsion angles, large fluctuations are observed for all concentration of cation studied here.

When the trajectories are analyzed in term of global shape, the effect of monovalent cation concentration is clarified (Fig. 2). In our previous exploration of UDP-Glc conformational space [4], the several overall shapes that could be adopted by the nucleotide-sugar were labeled according to their

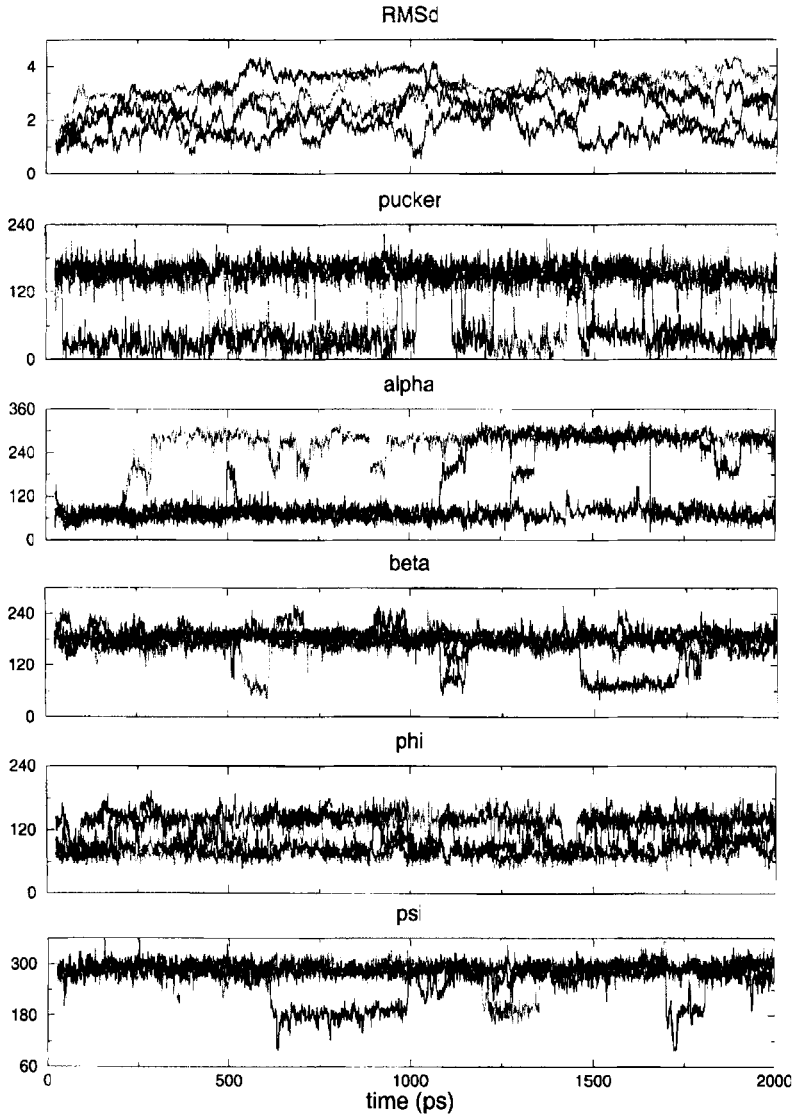

FIGURE 1 Comparison of heavy atom RMSds from starting structure (Å) and of torsion values (°) for several 2 ns trajectories of UDP-Glc in different concentration of K^+ ion: black: no salt, medium gray: LOW_K, light gray: MED_K and dark gray: HIGH_K. (See Color Plate VI).

TABLE II Time-averaged rms deviation (Å) during several MD simulations

Name of the simulation	*Base*	*Ribose*	*Diphosphate*	*Glucose*
NO	0.077	0.361	0.872	0.255
LOW_K	0.078	0.234	0.587	0.310
MED_K	0.078	0.400	0.798	0.304
HIGH_K	0.078	0.521	0.807	0.513

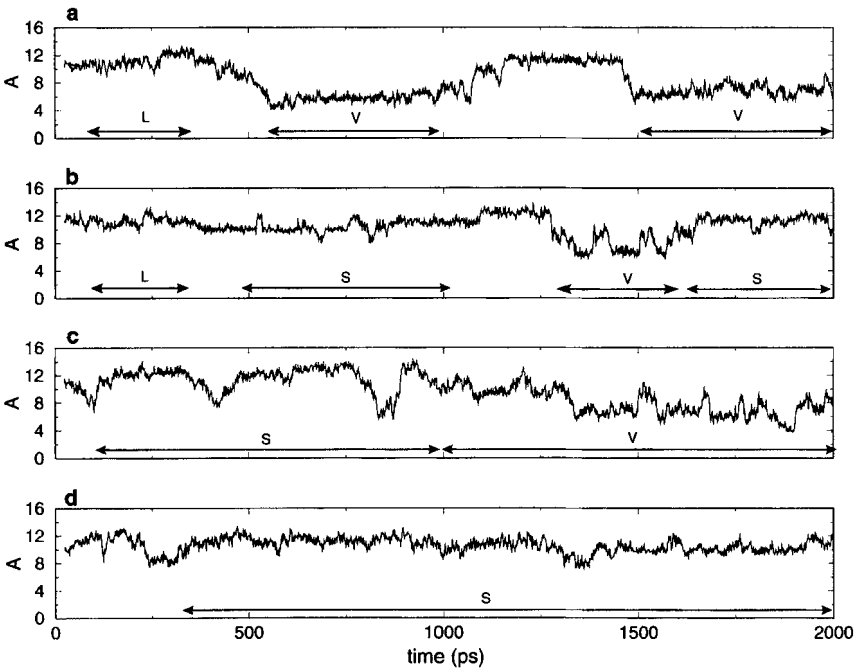

FIGURE 2 Distances between mass centers of uracile and glucose residues for no salt (a), LOW_K (b), MED_K (c) and HIGH_K (d) simulations. Arrows indicate intervals where the molecule adopts a conformation of V, L or S family.

resemblance with letter from the alphabet. In the present study, the starting L shape, a rather extended one that is observed in the crystal structure, is not stable in water environment and is lost after 300 ps or less. When no salt is present, this conformation exchanges with a V form that exhibits more intramolecular contact. It should be noted that in a previously calculated longer simulation (3 ns) in the absence of salt [4], the UDP-Glc molecule also explores the J shape, a different conformational family predicted in our preliminary conformational search [4]. The presence of salt induces the occurrence of a rather extended shape, *i.e.*, the S shape, that has the particularity to have the charged pyrophosphate oxygens on the most exposed side of the molecule. The interaction between negatively charged phosphate groups and positively charged potassium ion is then favored. Snapshots of representative conformations from each simulation are provided in Figure 3.

Table III displays some of the averaged distances measured during the simulation. It is clear that the more extended conformations, *i.e.*, the L shape of the crystal structure and the S shape predicted in high-salt concentration, are the ones that favor intermolecular contacts as compared to the

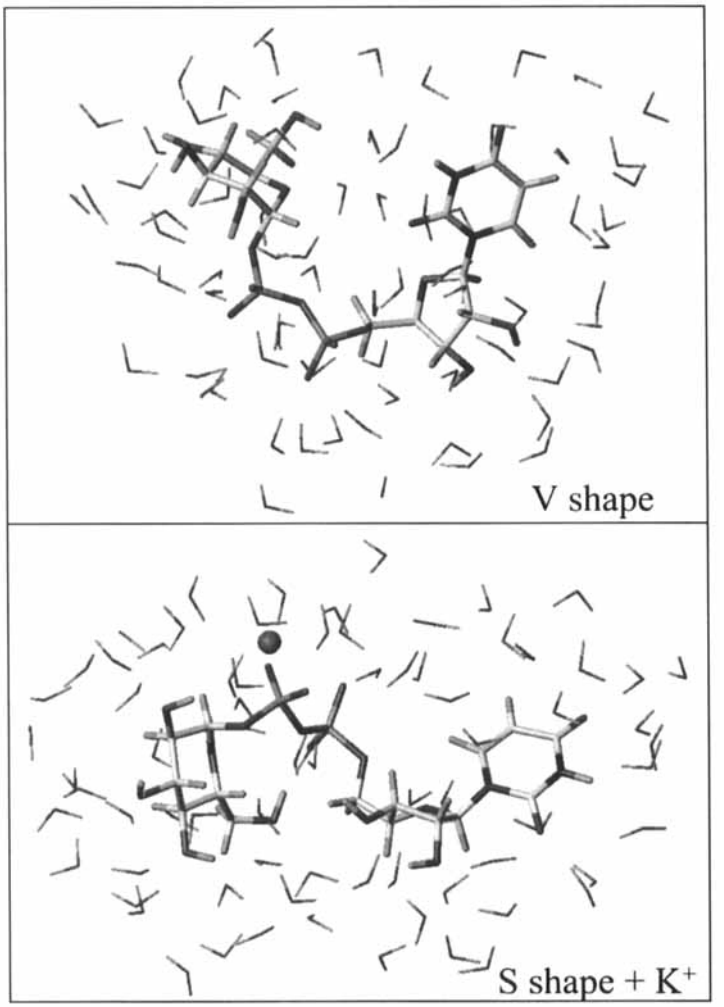

FIGURE 3 Snapshots from MED_K simulation with V family conformation and HIGH_K simulation with S family conformation including water molecules and K^+ ions in a 4 Å shell around the solute. (See Color Plate VII).

TABLE III Time-averaged distances (Å) between uracyl and glucose atoms for several MD simulations

	C1″ – N1	*C4″ – C4*	*O5″ – N3*
X-ray	8.4	11.5	10.8
NO	7.6	9.1	8.5
LOW_K	8.8	11.8	9.9
MED_K	8.3	10.6	9.2
HIGH_K	8.7	11.9	10.6

intramolecular interactions. These intermolecular contacts can be achieved either through packing interactions or phosphate-cation interactions.

Interaction Between UDP-Glc and Potassium Ions

The specific interaction between phosphate groups and cation can be analyzed by evaluating the radial distribution function $g(R)$ of K^+ around the two phosphorus atoms (Fig. 4). When performed at increasing salt concentrations, this function retains its bimodal aspect. The first peak of interaction is observed for a distance of 3.65 Å between P and K^+ whereas a second weaker peak appears at a distance of approx. 6 Å. The existence of the second peak could be due to (i) interaction of K^+ with the second phosphate (*i.e.*, when already interacting at 3.6 a with one of them) (ii) interaction screened by an hydration shell and (iii) interaction screened by other atoms of the UDP-Glc because of some particular conformation of the molecule.

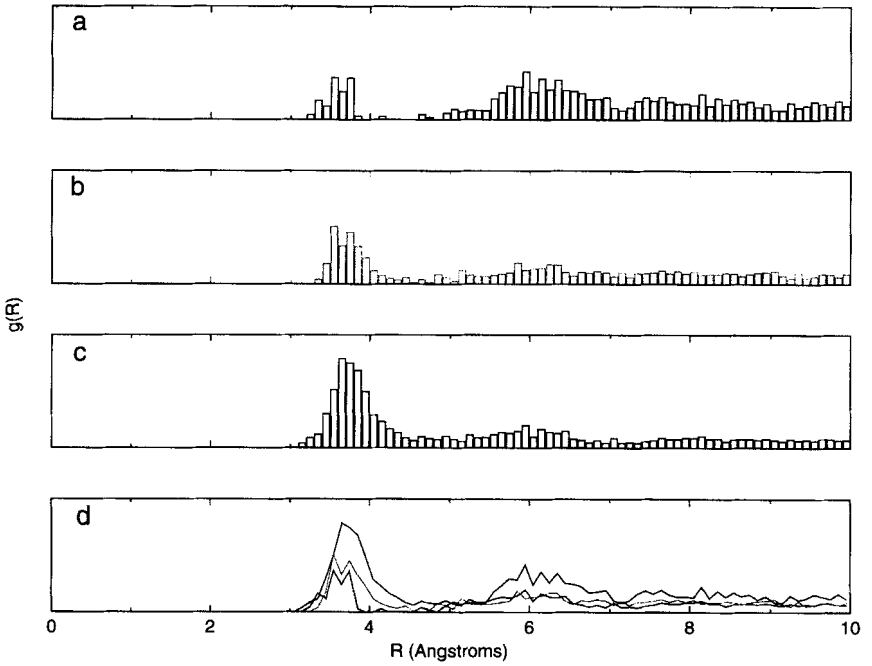

FIGURE 4 Radial distribution function (RDF) for the three K^+ concentrations: LOW_K (a and medium gray in d), MED_K (b and light gray in d) and HIGH_K (c and dark gray in d). The $g(R)$ is the volume-normalized density of ions counted in the distance R measured from the two phosphorus atoms of UDP-glucose. (See Color Plate VIII).

The radial pair distribution function was also calculated for the interaction of K^+ with oxygen atoms located in different part of the UDP-Glc molecule. The resulting $g(R)$ is displayed in Figure 5, after volume normalization. As expected, the K^+ ions interact preferentially with the negatively charged oxygen atoms of the phosphate groups. The maximum of interactions is at a distance of 2.65 Å. This short distance observed between charged oxygen and cation is in good agreement with the range 2.58 – 2.85 Å observed in crystal structure of nucleotide diphosphate potassium salt [17]. The potassium cation also interacts with oxygen in C(P)–O–C(P) sequences, that have also a non negligible negative charge, and with hydroxylic oxygens of the solute, and this with an optimal distance of 2.75 Å. Almost no short distance interactions are observed with oxygen atoms from the uridyl group. The $g(R)$ function is close to zero at a distance of 3.3 Å, indicating here the limit of the first shell of interaction between K^+ and UDP-Glc. A second interaction peak is observed at 4 Å for OS oxygen. This intermediate distance corresponds to K^+ interacting closely with charged phosphate

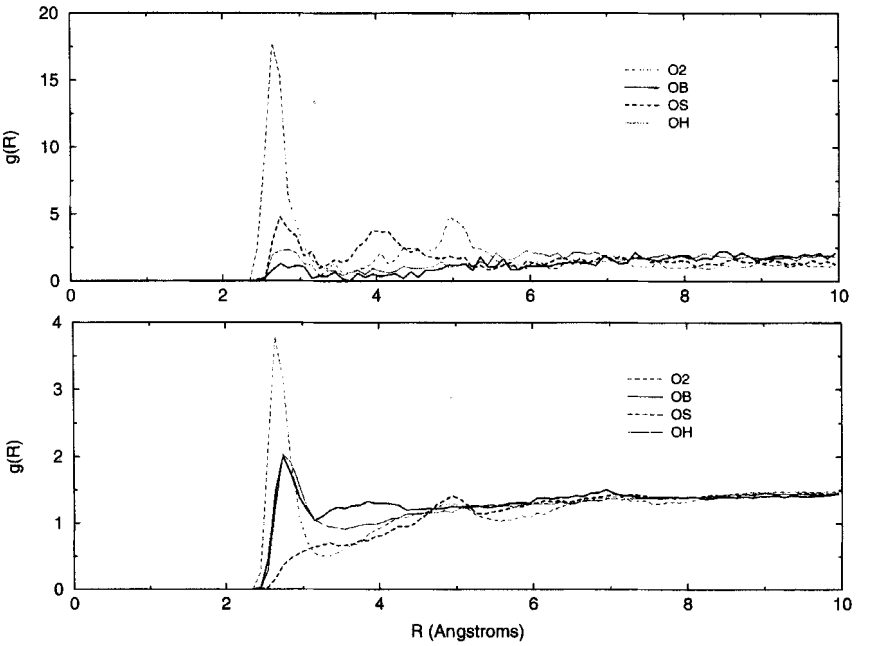

FIGURE 5 Volume-normalized radial distribution functions $g(R)$ of water oxygens (top) and K^+ ions (bottom) around solute oxygens calculated for HIGH_K simulations and partitioned along the solute oxygen types: O_2 (oxygens of P = O bonds), OB (carboxylic oxygens of base), OS (acetalic and esteric oxygens), OH (hydroxylic oxygens).

oxygens, and therefore brought close to pyrophosphate oxygen (C–O–P or P–O–P). The second maximum of the $g(R)$ function is at 5 Å for the interaction between K^+ for phosphate and base oxygen.

The analyses of the trajectories allow to examine all of the distances between potassium ions and charged oxygens, in order to know how many phosphate makes short contacts, and for how long (Fig. 6). Among the 12 potassium cations of the HIGH_K simulation, four establish contacts for significant periods of time with the phosphate groups, whereas four others are in contact with the phosphates only for very short time, and the four last are always in the outer shell. Examinations of the distance histories in Figure 6 indicate that our simulation is long enough to allow for cations to come close to the phosphate, leave apart, and come again. The several peaks of the radial pair distribution function can be correlated with the behavior of pairs of atoms: for example, when one K^+ makes electrostatic contact

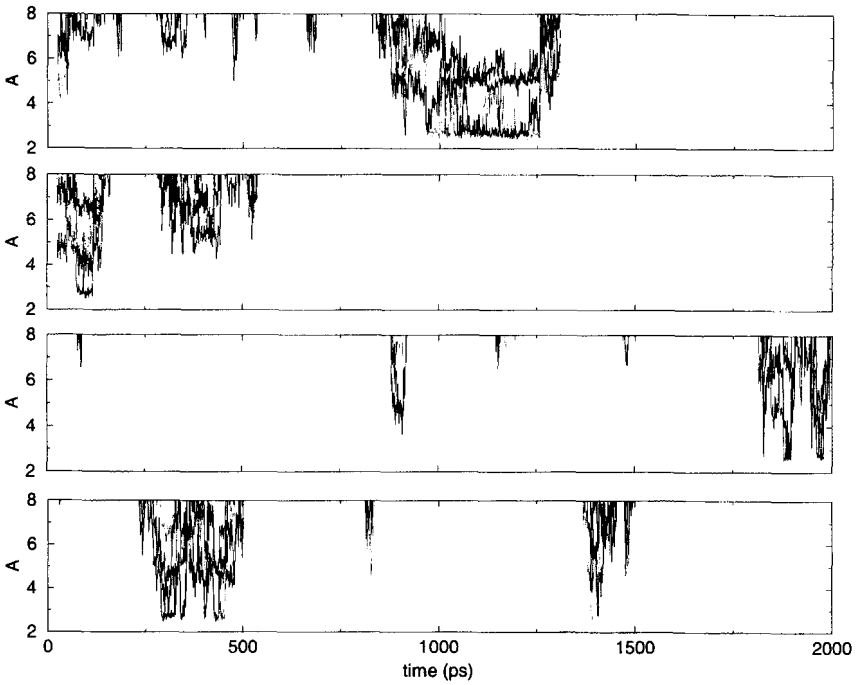

FIGURE 6 History of the distances between 4 of the 12 potassium cations and the charged phosphate oxygen atoms during the 2 ns trajectory of UDP-Glc performed in HIGH_K conditions. The four panels corresponds to four different potassium cations. Oxygens from phosphate groups have been color coded as follows: dark gray and medium gray for oxygen carried by the α-phosphate, light gray and dark gray for oxygen carried by the β-phosphate. (See Color Plate IX).

(2.65 Å) with the two oxygens of the α-phosphate, this brings this cation at 5 Å of the oxygen atoms of the β-phosphate, a distance that corresponds to the second peak of the radial distribution function. Analyses of the trajectories, together with calculation of the occupation numbers for potassium ion around the phosphate groups indicate that, even at high salt concentration, there is only zero or one (very rarely two or three) potassium ions in the first shell (<4 Å) around the phosphate groups.

Hydration Scheme

For the aim of comparison, the hydration scheme, *i.e.*, the radial pair distribution function of water molecules, has also been calculated (Fig. 5). Again, the shortest interaction occurs between water and charged phosphate oxygens at an optimum distance of 2.65 Å, whereas the interaction with neutral oxygen (hydroxyl of the carbohydrate moiety and carbonyl of the base moiety) occurs at 2.75 Å. Oxygen in C(P)–O–C(P) sequences are very poorly hydrated but present a but the $g(R)$ function present a peak corresponding to interaction with water at a distance of about 5 Å. The $g(R)$ functions can also been compared to those classically calculated for carbohydrates [18]. For sucrose simulation, the same radial hydration is observed for hydroxylic hydrogens.

Simulation in the Presence of Divalent Cation

Two simulations were conducted in presence of two different concentrations of magnesium ions (Tab. I). In both trajectories, the conformational behavior of UDP-Glc was completely different to what was observed during the trajectories in the presence of monovalent cation. In both LOW_Mg and MED_Mg trajectories, the UDP-Glc adopts a S shape after a few ps. This conformation is slightly more extended than the S-shape observed in the presence of potassium salt. Then the molecules did not show any more significant variations in conformation. It appears that the Mg^{2+} counterions interact very strongly with the charged phosphate oxygens and locks the molecule in this particular shape (Fig. 7).

The radial pair distribution function between Mg^{2+} ion and phosphorus atoms present two peaks: one at 3.35 Å and the second at 4.55 Å. This distribution function corresponds to a fixed position of the Mg^{2+} ion, strongly interacting with the β-phosphate, and at longer distance with the α one. In this energetically favored interaction, the distance between both β-phosphate oxygen atoms and the Mg^{2+} cation is about 2.0 Å, which is the

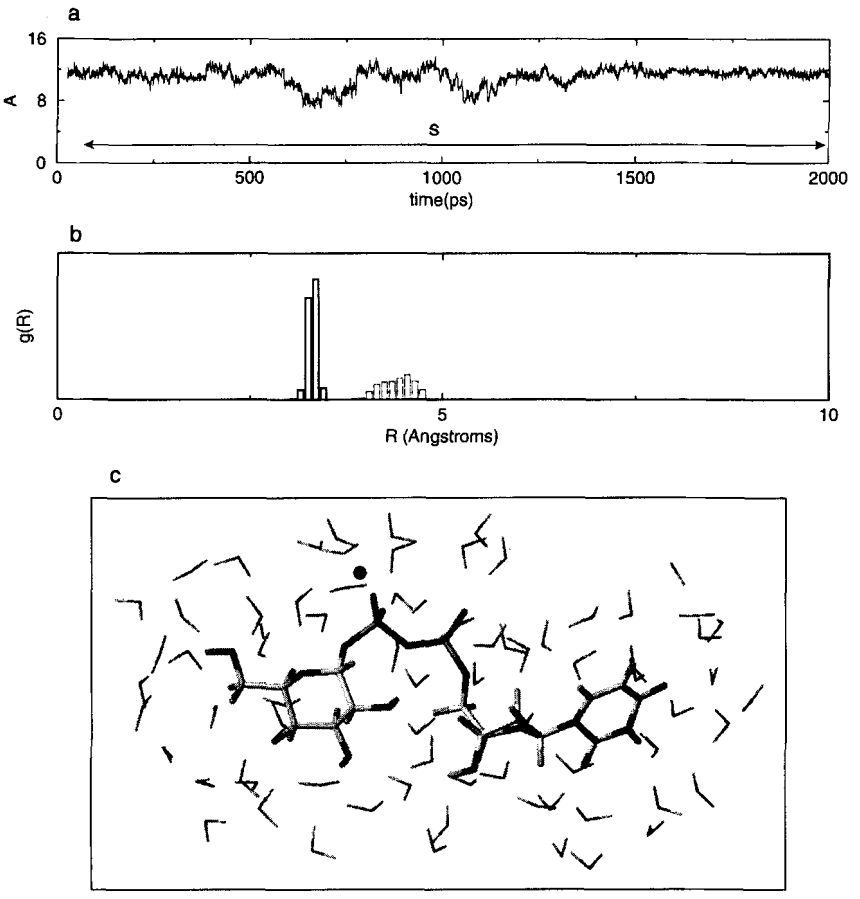

FIGURE 7 Analysis of the simulation of UDP-Glc in water with MED_Mg^{2+} conditions: (a) Distances between mass centers of uracile and glucose residues. Arrow indicates an interval when the molecule adopts a conformation of S family. (b) Radial distribution function (RDF) for Mg^{2+} ion. The $g(R)$ is the volume-normalized density of ion counted in the distance R measured from the two phosphorus atoms (light gray part from β-P and black part from α-P) of UDP-glucose. (c) Snapshots from Mg^{2+} simulations with S family conformation including water molecules water and Mg^{2+} ions in a 4 Å shell from the solute. (See Color Plate X).

distance measured in several crystals structure of magnesium salt of organic and inorganic pyrophosphate-containing molecules.

Evaluation of the occupation number indicate that even when several Mg^{2+} ions are present in the simulation, only one stays close to the UDP-Glc molecule. One has to be careful that no strong conclusion should be drawn from these simulations since not enough conformational space, or interaction modes, have been sampled due to the rigidity of the system.

DISCUSSION AND CONCLUSION

The present work described the first MD study of nucleotide-sugar in presence of cations. The conformational influence of increasing concentration of K^+ is of great interest. At high salt concentration, the molecule adopts an extended shape that allows for maximum interaction with the cations. However, the molecule is still very flexible and all of the torsional angles continue to vary, but always maintain an extended overall geometry. This flexibility is accompanied by large mobility of the K^+ ions that are not fixed in one site but move freely among the water molecules. The situation is completely different in the presence of divalent cations and our preliminary calculations indicate a rigid behavior of the molecule, that can no longer move once the Mg^{2+} cation is coordinated to the phosphate oxygens.

The simulations presented in the present work can be compared to the interaction classically described between nucleotide and cations. The stabilizing effects of cations on nucleic acid structures is generally described as 'counterion condensation' [19] in which anionic phosphodiester groups are electroneutralized by cations. These effects involve long-range electrostatic interactions between the polyanionic phosphodiester backbone and the condensed counterions. For the monovalent ions, two types of interactions with the solute are possible: a direct contact or interactions by hydration shell. The oxygen-cation distance in the K^+-DNA complex fluctuates between 2.45 and 3.81 Å [20]. As for divalent cation, the Mg^{2+}radial distribution function shows peaks at 3.35 and 4.85 Å from phosphorus atoms, which correspond to direct interactions and interactions *via* hydrated Mg^{2+} ions [21]. Experimental studies confirm that the majority of phosphate-Mg^{2+} interactions are performed by the primary hydration sphere of ion [21], although the direct contact between phosphate and divalent ion is also possible [22]. The divalent ions have water exchange times in the ns time and don't diffuse as rapidly as monovalents. The Mg^{2+} ions also decrease the mobility of the DNA phosphate backbone and water molecules hydrating the phosphate backbone. Increased salt concentrations leading to decreased water activity are generally considered to 'dehydrate' DNA.

It appears then that for monovalent cations, our MD simulation agrees well with what is already known for oligonucleotides. On the opposite, the preliminary calculations that we performed with divalent cations are in favor of a direct coordination of Mg^{2+} by the pyrophosphate oxygens, which seems to be a very different behavior that the one observed for phosphodiester linkage. When comparing the Mg^{2+}-phosphorus radial distribution function, pyrophosphate and phosphodiester linkages exhibit the

same strong interaction at 3.35 Å. However the second interaction peak is at 4.55 Å for pyrophosphate and 4.85 Å for phosphodiester. Therefore, it appears that the presence of diphosphate moiety induces a stronger interaction. It has already been observed that ADP forms 1:1/complexes with divalent metals [23].

This molecular modeling study opens a large number of question and perspectives and we envisage now, on one hand, to investigate in a more systematic way the possible interaction modes between nucleotide-sugars and divalent cations, and on the other hand to validate our simulations by high resolution nuclear magnetic resonance experiments.

Acknowledgments

P. P. was supported by a grant from the Ministère des Affaires Etrangères de la République Française. The research was partially supported by the Xenotransplantation Project BIO4CT972242 of the BIOTECH program from European Union (A.I.) and by grant No. VS96095 from the Ministry of Education of the Czeck Republic (J.K.). The authors are indebted to Kate Hervé du Penhoat for fruitful scientific discussions and correction of the manuscript and to Czeck Academic Supercomputer Center in Brno for providing access to computer facilities.

References

[1] (a) Neufeld, E. F. and Hassid, W. Z. (1963). "Biosynthesis of saccharides from glycopyranosyl esters of nucleotides", *Adv. Carbohydr. Chem. Biochem.*, **18**, 309. (b) Kotchekov, N. K. and Shibaev, V. N. (1973). "Glycosyl esters of nucleotide pyrophosphates", *Adv. Carbohydr. Chem. Biochem.*, **28**, 307. (c) Shibaev, V. N. (1986). "Biosynthesis of bacterial polysaccharide chains composed of repeating units", *Adv. Carbohydr. Chem. Biochem.*, **44**, 277.

[2] Kornfeld, R. and Kornfeld, S. (1985). "Assembly of asparagine-linked oligosaccharides", *Annu. Rev. Biochem.*, **54**, 631.

[3] Sugawara, Y. and Iwasaki, H. (1984)."Structure of disodium uridine diphosphoglucose dihydrate", *Acta Crystallogr.*, **C40**, 389.

[4] Petrova, P., Koca, J. and Imberty, A., "Potential energy hypersurfaces of nucleotide-sucres", *J. Am. Chem. Soc.*, **121**, 5535.

[5] Tvaroska, I., Andre, I. and Carver, J. P. (1999). "*Ab initio* molecular study of the conformational behavior of the sugar-phosphate linkage", *J. Phys. Chem. B*, **103**, 2560.

[6] Pearlman, D. A. *et al.* (1995). "AMBER, a package of computer programs", *Comp. Phys. Commun.*, **91**, 1.

[7] Case, D. A. *et al.* (1997). AMBER; 5.0 Ver., University of California, San Francisco.

[8] Koca, J. and Matyska, L. (1994). "Computer program CICADA–traveling along a conformational potential energy hypersurface", *J. Mol. Struct.* (THEOCHEM), **308**, 13.

[9] Murray, B. W., Takayama, S., Schultz, J. and Wong, C. H. (1996). "Mechanism and specificity of human a-1,3-fucosyltransferase V", *Biochemistry*, **34**, 11183.

[10] Busch, C., Hofmann, F., Selzer, J., Munro, S., Jeckel, D. and Aktories, K. (1998). "A common motif of eukaryotic glycosyltransferases is essential for the enzyme activity of large clostridial cytotoxins", *J. Biol. Chem.*, **273**, 19566.
[11] Breton, C., Bettler, E., Joziasse, D. H., Geremia, R. A. and Imberty, A. (1998). "Sequence-function relationships of procaryotic and eucaryotic galactosyltransferases", *J. Biochem.*, **123**, 1000.
[12] Imberty, A., Monier, C., Bettler, E., Morera, S., Freemont, P., Sippl, M., Flockner, H., Ruger, W. and Breton, C., "Fold recognition study of α-3-galactosyltransferase and molecular modeling of the nucleotide-sugar binding domain", *Glycobiology*, **9**, 713.
[13] Aqvist, J. (1990). "Ion-water interaction potentials derived from free energy perturbation simulations", *J. Phys. Chem.*, **94**, 8021.
[14] Ryckaert, J. P., Ciccotti, G. and Berendsen, H. J. C. (1977). "Numerical integration of the Cartesian equations of motion of a system with constrains: molecular dynamics of *n*-alkanes", *J. Comp. Phys.*, **23**, 327.
[15] Berendsen, H. J. C., Postma, J. P. M., van Gunsteren, W. F. and DiNola, A. (1984). "Molecular dynamics with coupling to an external bath", *J. Chem. Phys.*, **81**, 3684.
[16] Essmann, U., Petera, L., Berkowitz, M. L., Darden, T., Lee, H. and Pedersen, L. G. (1995). "A smooth particle mesh Ewald method", *J. Chem. Phys.*, **103**, 8577.
[17] Viswamitra, M. A., Seshadri, T. P., Hosur, M. V., Post, M. L. and Kennard, O. (1975). "An uncommon nucleotide conformation shown by molecular structure of deoxyuridine-5'-phosphate and nucleic acid stereochemistry", *Acta Crystallogr., Sect. A*, **31**, S45.
[18] Engelsen, S. B. and Perez, S. (1996). "The hydration of sucrose", *Carbohydr. Res.*, **292**, 21.
[19] Manning, G. S. (1978). "The molecular theory of polyelectrolyte solutions with applications to the electrostatic properties of polynucleotides", *Q. Rev. Biophys.*, **11**, 179.
[20] Ross, W. S. and Hardin, C. C. (1994). "Ion-induced stabilization of the G-DNA quadruplex: Free energy perturbation studies", *J. Am. Chem. Soc.*, **116**, 6070.
[21] MacKerell, A. D. Jr. (1997). "Influence of magnesium ions on duplex DNA structural, dynamic, and solvation properties", *J. Phys. Chem.*, **101**, 646.
[22] Buckin, V. A., Kankiya, B. I., Rentzeperis, D. and Marky, L. A. (1994). "Mg^{2+} recognizes the sequence of DNA through its hydration shell", *J. Am. Chem. Soc.*, **116**, 9423.
[23] Taqui Khan, M. M. and Martell, A. E. (1967). "Thermodynamic quantities associated with the interaction of adenosinediphosphoric and adenosinemonophosphoric acids with metal ions", *J. Am. Chem. Soc.*, **89**, 5585.